ISBN: 978-3-95450-223-3 ISSN: 2673-7000 doi:10.18429/JACoW-NAPAC2019-WEZBA3

# NO BEAM-LOSS QUADRUPOLE SCAN FOR TRANSVERSE PHASE SPACE MEASUREMENTS *

K. Fukushima†, T. Maruta, P. N. Ostroumov, T. Yoshimoto,
Facility for Rare Isotope Beams, Michigan State University, East Lansing, MI USA

## *Abstract*

Facility for Rare Isotope Beams (FRIB) at Michigan State University is based on a high power heavy ion linac and beam commissioning is under way. For evaluation of beam Twiss parameters and rms emittance, we routinely use multiple profile measurements while the strength of an upstream quadrupole is varied. The change of the quadrupole strength results in a beam mismatch downstream of the profile monitor which can cause beam losses. This is not acceptable in a high energy beamline. To avoid this transverse mismatch, we developed a beam matching procedure by optimization of quadrupoles' setting downstream of the profile monitor. Using this procedure we were able to eliminate beam losses during the quadrupole scan, and evaluate beam Twiss parameters and rms emittance. Examples of using this procedure in the folding segment of the FRIB linac are reported.

## INTRODUCTION

The driver linac of the Facility for Rare Isotope Beams (FRIB) is designed to accelerate stable ions from oxygen to uranium above 200 MeV/u [1]. Figure 1 shows the layout of the FRIB linac in the tunnel.

The linac segment 1 (LS1) was tuned for acceleration of argon beam up to 20.3 MeV/u [2, 3]. Other ion species such as Ne, Kr and Xe were accelerated to the same energy by simple scaling of all electromagnetic fields. The accelerated beams were stripped to higher charge states using the carbon foil and transported to the beam dump. The emittance growth on the stripping foil depends on the beam size and the beam phase space ellipse orientation on the stripper. Therefore, the transverse phase space measurements are necessary upstream of the stripper to optimize beam Twiss parameters on the stripper. A quadrupole-scan (Q-scan) method was applied to measure the beam Twiss parameters and emittance. Assuming a thin-lens model and a linear field beam optics, the root mean squared (rms) beam size at the downstream profile monitor can be written as a quadratic function of the upstream quadrupole strength and the transfer matrix elements between the quadrupole and the profile monitor. Even if we use a thick-lens beam optics model, we can obtain the beam $\sigma$-matrix by fitting the quadrupole strength to match the measured rms beam size. To achieve high accuracy of the Q-scan method the measured beam rms size as a function of the quadrupole strength should have downward-convex shape. The change of the quadrupole strength in the Q-scan procedure causes a significant beam mismatch in the downstream section and can result in beam losses. The latter can produce unnecessary radio-activation of the accelerator equipment. To avoid these beam losses, we developed a "Twiss recovery" procedure by optimization of the quadrupoles' setting downstream of the profile monitor.

## RMS ENVELOPES DURING Q-SCAN

Typically, the beam commissioning was performed using argon beam and Table 1 lists the design beam parameters at the exit of the last cryomodule in LS1.

Table 1: Design Beam Parameters at the Exit of the Last Cryomodule in LS1

| | | |
|---|---|---|
| Ion species | $^{40}\mathrm{Ar}^{9+}$ | |
| Beam energy [MeV/u] | 20.3 | |
| | $x$ | $y$ |
| Normalized rms emittance [$\pi$ mm-mrad] | 0.10 | 0.10 |
| Twiss parameter $\beta$ [m] | 5.0 | 5.0 |
| Twiss parameter $\alpha$ | 0.0 | 0.0 |

Figure 2 shows the layout of the optical elements and the design beam envelopes from the last cryomodule in the LS1 to the beam dump in the folding segment 1 (FS1). There are 16 quadrupoles upstream of the stripper, and last 4 quadrupoles are used for the beam matching to the stripper. The aperture radii are 25 mm at the quadrupoles and 17 mm at the rf bunchers. The first profile monitor is the most suitable for the quadrupole scan to obtain the downward-convex plot with a small range of the quadrupole strength variation.

Figure 3 presents the simulation results of the rms beam envelopes during the Q-scan for the 30 % variation of the quadrupole strength with respect to the design setting. The rms size difference in the vertical plane is large enough compared to the profile monitor accuracy. However, the rms beam envelopes downstream of the profile monitor are mismatched from the design envelopes especially in the vertical plane.

Figure 4 shows the rms beam envelope when we apply the "Twiss recovery" procedure downstream of the profile monitor. In this case, 4 quadrupoles between the profile monitor and the recovery point are optimized to reproduce the same Twiss parameters for each step of the Q-scan. As a consequence, the beam envelopes for each Q-scan quadrupole setting are recovered to match the design envelopes.

In operation, total 5 quadrupoles (1 for the Q-scan and 4 for the Twiss recovery) settings are pre-calculated using

---

* Work supported by the U.S. Department of Energy Office of Science under Cooperative Agreement DE-SC0000661, the State of Michigan and Michigan State University.

† fukushim@frib.msu.edu

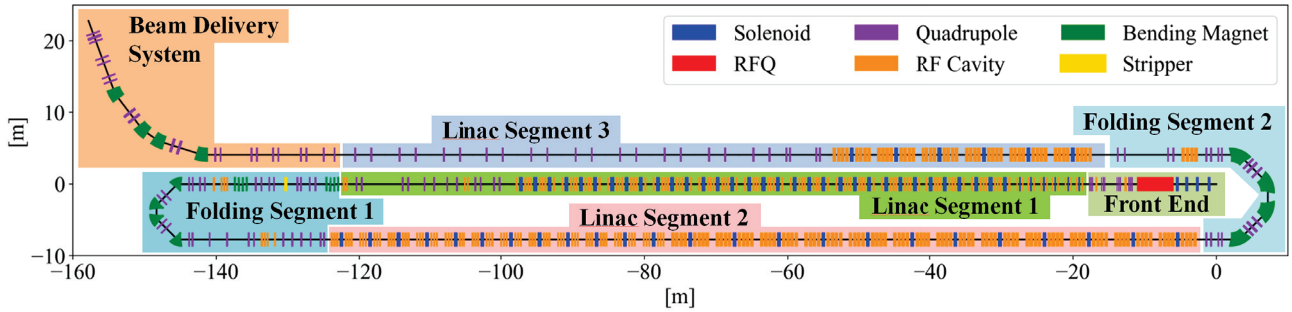

Figure 1: FRIB linac layout.

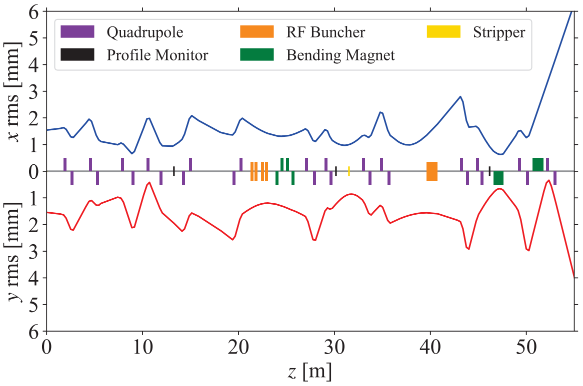

Figure 2: Design beam envelopes in the linac section from the last cryomodule to the beam dump in FS1.

the FLAME code [4–6], and all settings are applied simultaneously. FLAME is well suitable for this tuning purpose. The calculation time for the optimization of 4 quadrupoles setting for each profile measurement is approximately 0.1 s. Usually, we take 7 data points for one Q-scan procedure; therefore, we can find the Q-scan settings for the Twiss recovery within a second. The above Q-scan setting is most suitable for the measurements in one phase space plane (vertical plane in our case). Similarly, the measurements can be performed in other phase space plane with high accuracy by scanning another quadrupole.

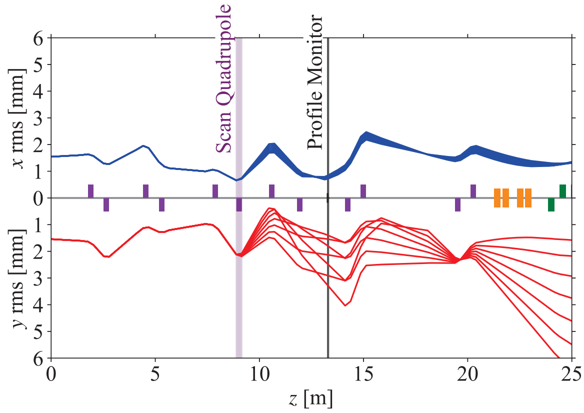

Figure 3: RMS beam envelopes during the Q-scan without Twiss recovery.

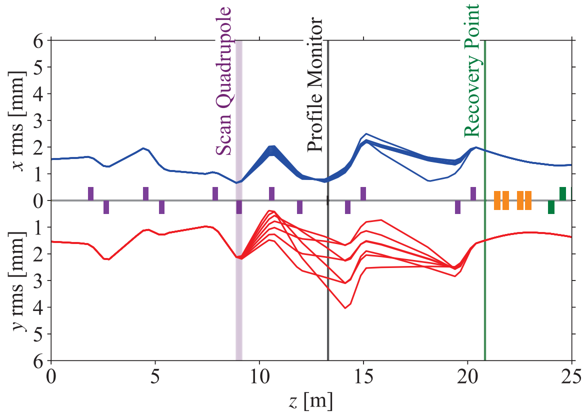

Figure 4: RMS beam envelopes during the Q-scan with Twiss recovery.

## EXPERIMENTAL RESULTS

Figure 5 presents the Q-scan measurement results with the Twiss recovery in FRIB FS1. The ion species and the beam energy are listed in Table 1. Here, we applied 2 cases of Q-scan procedure for precise phase space measurements in both vertical and horizontal planes. Figure 5 (a) corresponds to the Q-scan presented in Fig. 4, and Fig. 5 (b) shows the results of scanning of the next quadrupole of Fig. 5 (a). The same profile monitor is utilized for both cases. As we expected, the data points of the measured rms beam sizes are close to a quadratic function with respect to the quadrupole strength. The transverse 2nd order moments including the transverse coupling terms are evaluated by fitting both scan results simultaneously, and the fitting results are shown in Table 2. The difference between the design (dashed line) and fitting (solid line) in Fig. 5 corresponds to the difference of the design and measured beam parameters in Table 1 and Table 2. The measured beam Twiss parameters were utilized to control the beam phase space on the stripper.

In addition, Fig.6 shows the EPICS time log of the readbacks of the coil current of the quadrupole being scanned

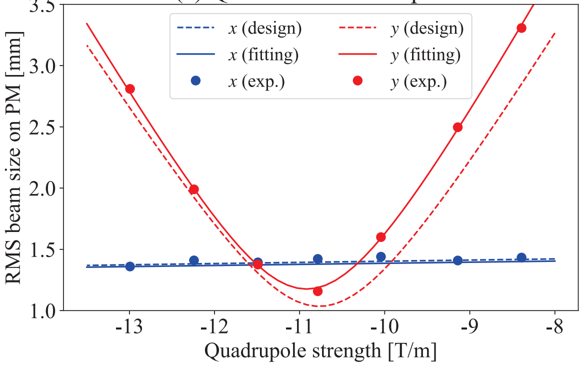
(a) Q-scan for vertical plane

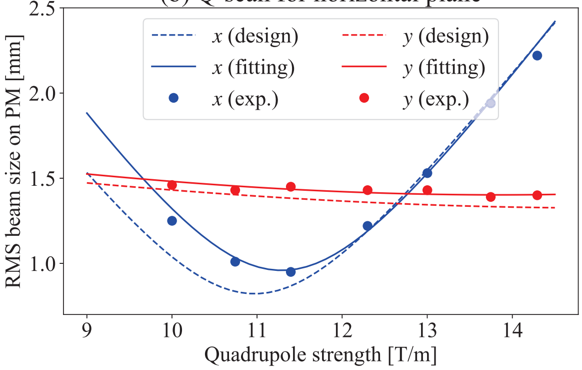
(b) Q-scan for horizontal plane

Figure 5: Experimental result of Q-scan with Twiss recovery. Upper figure (a) shows the experimental result of Q-scan for vertical plane measurement. The quadrupole settings are corresponds to the Q-scan of Fig. 4. Lower figure (b) is for horizontal plane measurement. In figure (b), we have scanned the next quadrupole of Fig. 4.

Table 2: Measured Beam Parameters at the Exit of the Last Cryomodule in LS1

| | $x$ | $y$ |
|---|---|---|
| Normalized rms emittance [$\pi$ mm-mrad] | 0.13 | 0.13 |
| Twiss parameter $\beta$ [m] | 4.0 | 5.9 |
| Twiss parameter $\alpha$ | 0.13 | -0.02 |

and the beam current monitors (BCM). Upper line corresponds to the quadrupole strength (purple line), and it is changed due to the Q-scan steps. Lower lines are the BCM signals at the LS1 entrance (green line) and the FS1 beam dump (blue). The BCM signals are averaged within a second. The BCM signals for both LS1 entrance and FS1 beam dump are almost overlapped during the Q-scan with Twiss recovery. The spike noises of the BCM signals at FS1 beam dump (blue line) are caused by the insertion of the profile monitor's wire. Normally, the beam centroid trajectory is not in the center of the quadrupole, hence the beam central trajectory also changes during the Q-scan.

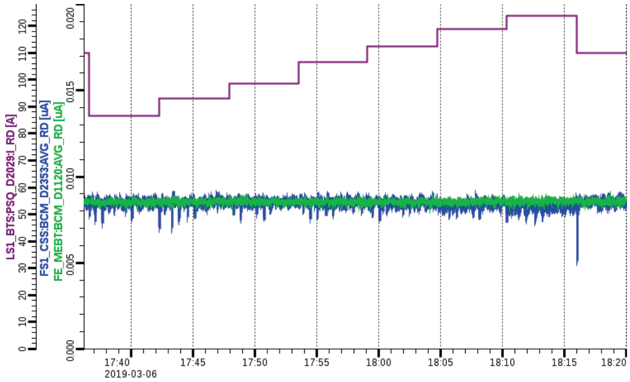

Figure 6: Screenshot of EPICS readback log during the Q-scan with Twiss recovery. Upper line corresponds to the quadrupole strength (purple). Lower lines are the readback of BCM at LS1 entrance (green) and BCM at FS1 beam dump (blue).

## CONCLUSION

In FS1 section of the FRIB linac, the transverse Twiss parameters and rms emittances were measured without generation of any beam losses by using Q-scan with Twiss recovery procedure. The FLAME code reproduces the experimental results well, and this fast optimization routine is useful for beam tuning. The Twiss recovery procedure is a very useful method to avoid unnecessary beam losses and activation of the accelerator equipment during Q-scan measurements.

## REFERENCES

[1] J. Wei *et al.*, "Advances of the FRIB project," *Int. J. Mod. Phys. E*, vol. 28, p. 1930003, 2019.

[2] P. N. Ostroumov *et al.*, "Heavy ion beam acceleration in the first three cryomodules at the Facility for Rare Isotope Beams at Michigan State University," *Phys. Rev. Accel. Beams*, vol. 22, p. 040101, 2019.

[3] P. N. Ostroumov *et al.*, "Beam commissioning in the first superconducting segment of the Facility for Rare Isotope Beams," *Phys. Rev. Accel. Beams*, vol. 22, p. 080101, 2019.

[4] Z. He, Y. Zhang, J. Wei, Z. Liu, and R. M. Talman, "Linear Envelope Model for Multicharge State Linac," *Phys. Rev. ST Accel. Beams*, vol. 17, p. 034001, 2014.

[5] Z. He, M. Davidsaver, K. Fukushima, G. Shen, M. Ikegami, and J. Bengtsson, "The fast linear accelerator modeling engine for FRIB online model service," *Computer Physics Communications*, vol. 234, pp. 167-178, 2019.

[6] FLAME source code repository, `https://github.com/frib-high-level-controls/FLAME`.